THE JOURNAL OF BIOLOGICAL CHEMISTRY VOL. 291, NO. 19, pp. 10201–10209, May 6, 2016

Deletions of Retinoblastoma 1 (*Rb1*) and Its Repressing Target S Phase Kinase-associated protein 2 (*Skp2*) Are Synthetic Lethal in Mouse Embryogenesis*

Received for publication, January 26, 2016, and in revised form, March 8, 2016 Published, JBC Papers in Press, March 10, 2016, DOI 10.1074/jbc.M116.718049

Hongling Zhao[1], **Hongbo Wang**[2], **Frederick Bauzon, Zhonglei Lu, Hao Fu, Jinhua Cui, and Liang Zhu**[3]

From the Department of Developmental and Molecular Biology, and Ophthalmology & Visual Sciences, and Medicine, The Albert Einstein Comprehensive Cancer Center and Liver Research Center, Albert Einstein College of Medicine, Bronx, New York 10461

Tumor suppressor pRb represses Skp2, a substrate-recruiting subunit of the SCF^{Skp2} ubiquitin ligase. $Rb1^{+/-}$ mice incur "two-hit" pituitary tumorigenesis; $Skp2^{-/-};Rb1^{+/-}$ mice do not. $Rb1^{-/-}$ embryos die on embryonic day (E) 14.5–15.5. Here, we report that $Skp2^{-/-};Rb1^{-/-}$ embryos died on E11.5, establishing an organismal level synthetic lethal relationship between *Rb1* and *Skp2*. On E10.5, $Rb1^{-/-}$ placentas showed similarly active proliferation and similarly inactive apoptosis as WT placenta, whereas $Rb1^{-/-}$ embryos showed ectopic proliferation without increased apoptosis in the brain. Combining $Skp2^{-/-}$ did not reduce proliferation or increase apoptosis in the placentas but induced extensive apoptosis in the brain. We conditionally deleted *Rb1* in neuronal lineage with Nes-Cre and reproduced the brain apoptosis in E13.5 Nes-Cre;$Rb1^{lox/lox};Skp2^{-/-}$ embryos, demonstrating their synthetic lethal relationship at a cell autonomous level. Nes-Cre-mediated *Rb1* deletion increased expression of proliferative E2F target genes in the brains of $Skp2^{+/+}$ embryos; the increases rose higher with activation of expression of apoptotic E2F target genes in $Skp2^{-/-}$ embryos. The brain apoptosis was independent of p53 but coincident with proliferation. The highly activated expression of proliferative and apoptotic E2F target genes subsided with gradually reduced roles of Skp2 in preventing p27 protein accumulation in the brain in late gestation, allowing the embryos to reach full term with normally sized brains. These findings establish that *Rb1* and *Skp2* deletions are synthetic lethal and suggest how this lethal relationship might be circumvented, which could help design better therapies for pRb-deficient cancer.

Children who inherit one null allele of the retinoblastoma 1 gene (*RB1*) are $RB1^{+/-}$ in all cells and develop retinoblastoma with full penetrance, and the retinoblastoma cells are invariably $RB1^{-/-}$. These cases represent the classic "two-hit" *RB1*-deficient tumorigenesis. Mice that inherited one knock-out allele of *Rb1* (the mouse homolog of *RB1*) are $Rb1^{+/-}$ in all cells and develop pituitary melanotroph tumors with full penetrance, and the tumor cells are invariably $Rb1^{-/-}$. $Rb1^{+/-}$ mice therefore model the two-hit *RB1*-deficient tumorigenesis. Biochemical studies have identified many repressing targets of pRb (encoded by *RB1*), with E2F1, E2F2, and E2F3 being the best studied (1). It is hypothesized that *RB1*-deficient tumorigenesis is caused by abnormal activation of pRb repressing targets following the inactivation of pRB. When $Rb1^{+/-}$ mice were used to test this hypothesis, the combined deletion of *E2f1* (2) or *E2f3* (3) inhibited pituitary tumorigenesis in $Rb1^{+/-}$ mice to various degrees.

pRb represses Skp2 by inhibiting its binding to p27 (4), reducing its mRNA expression via E2F (5, 6), and promoting its degradation via APC/C (7). Combined deletion of *Skp2* inhibited pituitary melanotroph tumorigenesis in $Rb1^{+/-}$ mice, establishing Skp2 as a functionally significant pRb repressing target in two-hit *Rb1*-deficient tumorigenesis. Remarkably, whereas combined deletion of pRb repressing targets *E2f1* (2), *E2f3* (3), and *Id2* (8) slowed pituitary tumorigenesis and extended the survival of $Rb1^{+/-}$ mice by a few months, pituitary of $Skp2^{-/-};Rb1^{+/-}$ mice were free of oncogenic lesions at 17 months of age when littermate $Skp2^{+/+};Rb1^{+/-}$ mice all died of pituitary tumors before 13 months of age. Artificial deletion of *Rb1* in melanotrophs by Pomc-Cre revealed apoptosis in pituitary intermediate lobe in 10-day-old $Skp2^{-/-}$;*Pomc-Cre;* $Rb1^{lox/lox}$ mice and reduction of the intermediate lobe to a layer one cell thick by 7 weeks of age. These observations suggest a survival role of Skp2 in *Rb1*-deficient melanotroph tumorigenesis, shedding light on how $Skp2^{-/-}$ prevents pituitary tumorigenesis in $Skp2^{-/-};Rb1^{+/-}$ mice.

Rb1 is an essential gene in mouse embryogenesis, because $Rb1^{-/-}$ embryogenesis becomes lethal on embryonic day 14.5–15.5 (E14.5–15.4)[4] (9–11). $Rb1^{-/-}$ embryogenesis provides another experimental system to test the functional significance of biochemically identified pRb repressing targets. In previous studies, when deletion of a pRb repressing target inhibited pituitary tumorigenesis in $Rb1^{+/-}$ mice, the same deletion extended survival of $Rb1^{-/-}$ embryogenesis (12–14). A

* This work was supported by National Institutes of Health Grants RO1CA127901and RO1CA131421 (to L. Z.), Albert Einstein Comprehensive Cancer Research Center Grant 5P30CA13330, and Liver Research Center Grant 5P30DK061153. The authors declare that they have no conflicts of interest with the contents of this article.

[1] Recipient of Department of Defense Prostate Cancer Research Program (PCRP) Postdoctoral Fellowship PC121837.

[2] Present address: Dept. of Pathology, University of Texas Health Science Center, San Antonio, TX 78229.

[3] Irma T. Hirschl Career Scientist Award recipient. To whom correspondence should be addressed: Dept. of Developmental and Molecular Biology, Albert Einstein College of Medicine, 1300 Morris Park Ave., Rm. U-521, Bronx, NY 10461. Tel.: 718-430-3320; Fax: 718-430-8975; E-mail: liang.zhu@einstein.yu.edu.

[4] The abbreviations used are: E*n*, embryonic day *n*; IHC, immunohistochemistry; IF, immunofluorescence; PCNA, proliferating cell nuclear antigen; qPCR, quantitative PCR; H&E, hematoxylin and eosin.

straightforward paradigm therefore emerged: if a biochemically identified pRb repressing target is functionally significant, its deletion would lessen the effects of *Rb1* inactivation, manifested as inhibition of pituitary tumorigenesis to extend survival of $Rb1^{+/-}$ mice and correction of defects in $Rb1^{-/-}$ embryogenesis to extend survival of $Rb1^{-/-}$ embryos. In the current study, we determined how Skp2, whose deletion more effectively inhibited pituitary tumorigenesis in $Rb1^{+/-}$ mice than all other pRb repressing targets tested so far, fits into this paradigm.

Experimental Procedures

Mice—Nes-Cre mice were obtained from The Jackson Laboratory. $Rb1^{+/-}$ (9), $Rb1^{lox/lox}$ (15), $Skp2^{-/-}$ (16), and $Trp53^{lox/lox}$ mice (17) have been described. Nes-Cre was genotyped using primers Cre F (5′-ATGCCCAAGAAGAAGAGGAAGGT-3′) and Cre R (5′-GAAATCAGTGCGTTCGAACG CTAGA-3′). Other genotyping details were previously described (18, 19). The mice used in this study were on mixed C57BL/6J×129Sv×FVB strain background. The mice were maintained under pathogen-free conditions in the Albert Einstein College of Medicine animal facility. All procedures were reviewed and approved by Einstein Animal Care Committee, conforming to accepted standards of humane animal care.

Embryos Gestation Determination and Analyses—Gestation and embryo age were determined by timed mating. Male and female mice were put in the same cage in late evening on day 1 and were separated in early morning on day 2. The embryo age was counted as E0.5 on day 2 if the female mice were found pregnant later. Pregnant females were intraperitoneally injected with BrdU (0.1 mg/g) 2 h before harvest. Embryos at various ages were harvested and were fixed in 10% formalin (Fisher Scientific, SF 100-4), embedded in paraffin wax, and sectioned. For embryos older than E15.5, decalcification was performed before routine processing to paraffin embedding. Embryo histology studies were conducted together with Albert Einstein Cancer Center mouse pathology core. Embryo brains used for RT-PCR and Western blots were dissected, snap frozen, and kept in −80 °C freezer.

Immunohistochemistry (IHC), Immunofluorescence (IF) Staining, and Microscopy—For IHC and IF staining, embryos were sectioned at 5-μm thickness. The slides were deparaffinized, hydrated, and incubated in a steamer for 20 min in sodium citrate buffer (Vector Labs, H3301) for antigen retrieval. Sections were first treated with 3% H_2O_2 to quench endogenous peroxidase, washed several times, blocked with 10% normal goat serum, and then incubated in primary antibodies at 4 °C overnight. The following antibodies were used: BrdU (CalBiochem, NA61, 1:100 dilution), PCNA (Santa Cruz Biotechnology, sc-56, 1:100 dilution), and aCasp3 (Cell Signaling Technology, 9664S, 1:100 dilution). SuperPicture™ kit (Invitrogen, 879263 and 879163) was used to detect signals in IHC staining. IF detection of PCNA was done with rhodamine-labeled goat anti-mouse IgG (Thermo Scientific, 31660, 1:100 dilution), aCasp3 was detected by TSA™PLUS fluorescence kit (NEL741001KT, PerkinElmer Life Science), and TUNEL staining was performed with an apoptosis detection kit (Millipore, S7100 and S7110). IHC staining was counterstained with Harris Hematoxylin (Poly Scientific R&D Corp, S212), and IF staining was counterstained with DAPI (Sigma-Aldrich, D-9564). The images were visualized with a Nikon Eclipse Ti-U microscope, captured with Olympus DP71 camera and DP Controller software (3.2.1.276), and saved with DP manager software (3.1.1.208). The images were further processed by Adobe Photoshop. For BrdU and TUNEL staining quantification, pictures were taken under 400× magnificence. Approximately 400–500 total cells were counted in each sample.

RT-qPCR and Western Blots—For RT-qPCR analyses, total RNA was isolated from indicated embryo brains with RNeasy kit (Qiagen), and 2.5 μg of RNA was reverse transcribed to cDNA in a 20-μl reaction with Superscript first strand synthesis system (Invitrogen). After 20 times dilution, ~2 μl of cDNA of each sample was used as template for real time PCRs using SYBR Green dye (Applied Biosystems). All RT-qPCR results were normalized with GAPDH in the same samples and presented as the average of results from at least three embryo brains for each genotype. The primers for RT-qPCR were described before (20). For Western blot analyses, embryo brains were homogenized with Dounce glass homogenizer in radioimmune precipitation assay buffer. Protein concentrations were determined by Bio-Rad protein assay kit (catalog no. 500-0006) using a SmartSpec™ 3000 spectrophotometer for equal loading by protein content. The same amount of protein extract was loaded on SDS gel, blotted, and probed with the following antibodies: pRb (BD Pharmingen, 554136, 1:1000 dilution), PCNA (Santa Cruz Biotechnology, sc-56, 1:500 dilution), E2F1 (Santa Cruz Biotechnology, sc-193, 1:200 dilution), Cyclin A (Santa Cruz Biotechnology, sc-751, 1:200 dilution), Cyclin E (Santa Cruz Biotechnology, sc-481, 1:200 dilution), Skp2 (Santa Cruz Biotechnology, sc-7164, 1:200 dilution), p73 (Abcam, ab40658, 1:1000 dilution), phosphorylated-Histon H3 (Cell Signaling, 9701L, 1:1000 dilution), aCasp3 (Cell Signaling Technology, 9664S, 1:1000 dilution), p27 (BD Transduction Lab, 610242, 1:1000 dilution), and Tubulin (Sigma-Aldrich, T6074, 1:5000 dilution). 8% SDS-PAGE gel was used for pRb protein analysis, 12% gels were used for pHH3 and aCasp3 analyses, and 10% gels were used for other protein analyses. The protein marker for Western blot was from Crystalgen Inc. (catalog no. 65-0671). At least three embryo brains of indicated genotypes at different embryonic stages were analyzed with highly reproducible results.

Statistical Analysis—Differences in BrdU, TUNEL labeling, and RT-qPCR between indicated samples were analyzed by two-sided Student's *t* test. $p < 0.05$ is considered as statistically significant. Embryo survival analyses were analyzed by Fisher's exact test (*, $p < 0.05$; **, $p < 0.01$; ***, $p < 0.005$).

Results

$Skp2^{-/-};Rb1^{-/-}$ Embryogenesis Is Lethal on E11.5—To define functional relationships between $Skp2^{-/-}$ and $Rb1^{-/-}$ in embryogenesis, we mated $Skp2^{+/-};Rb1^{+/-}$ mice to combine $Skp2^{-/-}$ and $Rb1^{-/-}$ in embryogenesis. $Skp2^{-/-}$ mice are viable with normal life span (16), whereas $Rb1^{-/-}$ embryos die on E14.5-E15.5 (9–11). Table 1 shows the survival and death (presence or absence of a beating heart) of three key genotypes (WT, $Rb1^{-/-}$, and $Skp2^{-/-};Rb1^{-/-}$) between E10.5 and E13.5. We

found dead $Rb1^{-/-}$ embryos at low frequencies on E10.5 (1 of 19), E11.5 (2 of 19), E12.5 (0 of 9), and E13.5 (1 of 7). These low frequencies increased to 1 of 8, 9 of 16, 3 of 4, and 5 of 5, respectively, in $Skp2^{-/-};Rb1^{-/-}$ embryos. The increases are statistically significant on E11.5 ($p = 0.0088$), E12.5 ($p = 0.014$), and E13.5 ($p = 0.015$). Thus, $Skp2^{-/-}$ and $Rb1^{-/-}$ are synthetic lethal at the organismal level in mouse embryogenesis.

TABLE 1

$Skp2^{-/-};Rb1^{-/-}$ embryogenesis becomes lethal on E11.5

Mating was between $Skp2^{+/-};Rb1^{+/-}$ mice. Total numbers of embryos harvested (total column) on each gestational day (age) are shown. Total and dead (in parentheses) numbers for the three key genotypes are shown. Death was defined as absence of heart beat. *p* values compare lethality of $Rb1^{-/-}$ versus $Skp2^{-/-};Rb1^{-/-}$ embryos (see text for more details).

Age	Total	$Skp2^{+/+}$; $Rb1^{+/+}$	$Skp2^{+/+}$; $Rb1^{-/-}$	$Skp2^{-/-}$; $Rb1^{-/-}$	*p* values
E10.5	148	10 (0)	19 (1)	8 (1)	$p = 1.000$
E11.5	197	16 (0)	19 (2)	16 (9)	$p = 0.009$
E12.5	116	3 (0)	9 (0)	4 (3)	$p = 0.014$
E13.5	120	5 (0)	7 (1)	5 (5)	$p = 0.015$

$Skp2^{-/-}$ Induces Apoptosis in Brains of E10.5 $Skp2^{-/-};Rb1^{-/-}$ Embryos—Lethality in $Rb1^{-/-}$ embryogenesis on E14.5-E15.5 is caused by placental defects. Leone and co-workers (11, 21) showed that WT and $Rb1^{-/-}$ placentas were similarly highly proliferative on E11.5, but proliferation failed to decrease in $Rb1^{-/-}$ placenta compared with WT placenta on E13.5, leading to overexpansion of trophoblasts in labyrinth layer, which clogs mother-fetus exchange. Because 60% of $Skp2^{-/-};Rb1^{-/-}$ embryos were dead on E11.5, we examined proliferation and apoptosis of placentas of the four combinations of *Skp2* and *Rb1* genotypes ($Skp2^{+/+};Rb1^{+/+}$, $Skp2^{+/+};Rb1^{-/-}$, $Skp2^{-/-};Rb1^{+/+}$, and $Skp2^{-/-};Rb1^{-/-}$) on E10.5. We found indistinguishable high proliferation (Fig. 1, *A* and *C*) and low apoptosis (Fig. 1, *B* and *D*) among these four genotypes. The structural defect of $Rb1^{-/-}$ placenta on E13.5 is clumps of trophoblasts in the labyrinth layer to the extent that restricted mother-fetus exchange space. On E10.5, trophoblasts clumps can be found in the labyrinth layer of WT and $Skp2^{-/-}$ placentas, likely because of the high proliferation in this location at

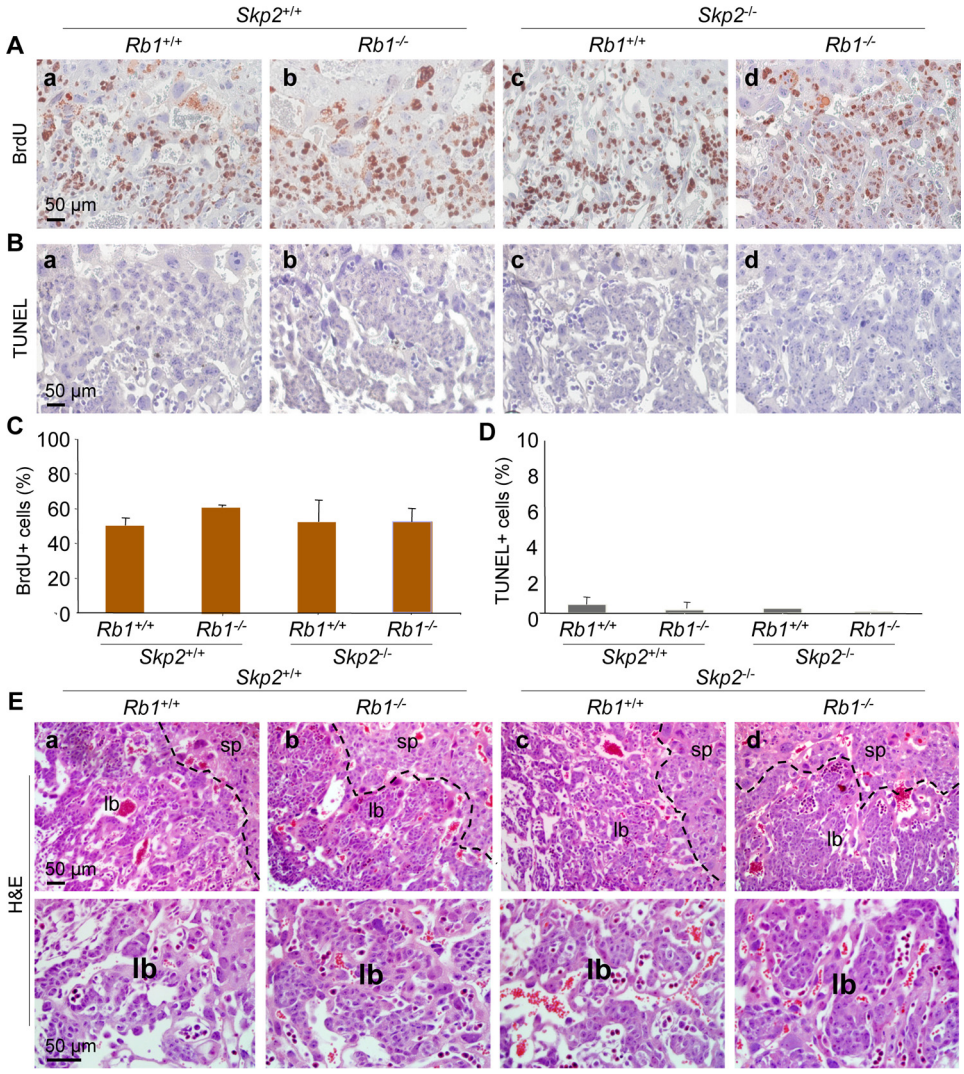

FIGURE 1. **Indistinguishable high proliferation and low apoptosis in $Skp2^{+/+};Rb1^{+/+}$, $Skp2^{+/+};Rb1^{-/-}$, $Skp2^{-/-};Rb1^{+/+}$, and $Skp2^{-/-};Rb1^{-/-}$ placentas on E10.5.** *A–D*, BrdU labeling (*A*) and TUNEL staining (*B*) of E10.5 placentas of the indicated genotypes, and their quantification (*C* and *D*). *E*, representative H&E staining of the indicated E10.5 placentas showing both the spongiotrophoblast layer (*sp*) and labyrinth layer (*lb*) separated by *dashed lines* (*upper row*) and trophoblast clumps in the labyrinth layer (*lower row*).

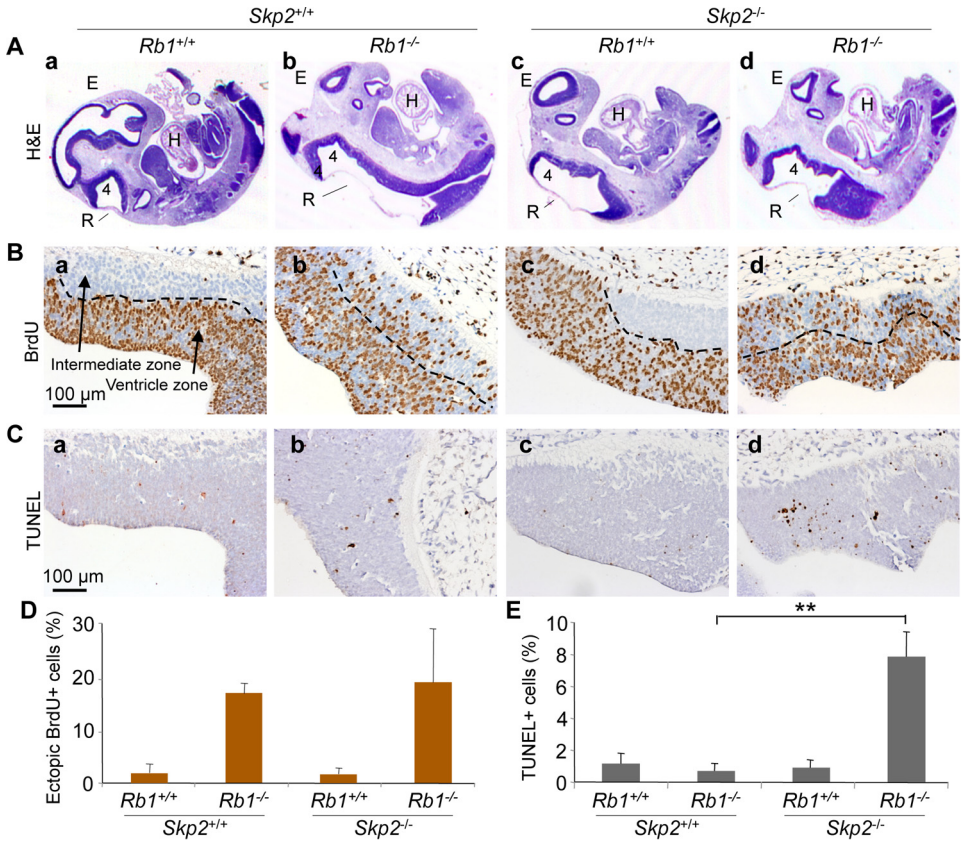

FIGURE 2. **Apoptosis in developing brains of E10. 5 *Skp2*$^{-/-}$;*Rb1*$^{-/-}$ embryos.** *A*, scan images of H&E-stained whole embryo sections of indicated genotypes. Certain organogenesis landmarks are marked: *E* (encephalic vesicles), *R* (roof of hindbrain), *4* (fourth ventricle), and *H* (heart). *B* and *D*, BrdU labeling showing ectopic proliferation in the intermediate zone of neuroepithelium of the developing brains in *Skp2*$^{+/+}$;*Rb1*$^{-/-}$ and *Skp2*$^{-/-}$;*Rb1*$^{-/-}$ E10.5 embryos (*B*), quantified in *D*. *C* and *E*, TUNEL staining of neuroepithelium in the same set of embryos (*C*) and quantified in *E*. Quantification included data from three sets of embryos. Statistical analyses were performed by Student's *t* test. **, $p = 0.002$.

this gestational stage. In comparison to WT and *Skp2*$^{-/-}$ placentas, *Rb1*$^{-/-}$ and *Skp2*$^{-/-}$;*Rb1*$^{-/-}$ placentas showed noticeably larger trophoblast clumps (Fig. 1*E*). In the embryo proper, the four genotypes showed comparable organogenesis at E10.5 of heart (Fig. 2*A*, marked as *H*) and the central nervous system showing encephalic vesicles (Fig. 2*A*, marked as *E*), roof of hindbrain (Fig. 2*A*, marked as *R*), and fourth ventricle (Fig. 2*A*, marked as *4*). Upon BrdU labeling, *Rb1*$^{-/-}$ embryos (*Skp2*$^{+/+}$ or *Skp2*$^{-/-}$) showed ectopic proliferation in the intermediate zone of the neuroepithelium in the developing brain (Fig. 2, *B* and *D*), and these brain regions in *Skp2*$^{-/-}$;*Rb1*$^{-/-}$ embryos further contained significant TUNEL staining (Fig. 2, *C* and *E*). Thus, the *Skp2-Rb1* synthetic lethal relationship is present at a cellular level as neuronal apoptosis in E10.5 *Skp2*$^{-/-}$;*Rb1*$^{-/-}$ embryos, but not in E10.5 *Rb1*$^{-/-}$ or E10.5 *Skp2*$^{-/-}$ embryos.

Rb1 Deletion in Neuronal Lineage Defines the Skp2-Rb1 Synthetic Lethal Neuronal Apoptosis as Cell Autonomous—To determine whether the neuroepithelium apoptosis in E10.5 *Skp2*$^{-/-}$;*Rb1*$^{-/-}$ embryos implicated a cell autonomous *Skp2-Rb1* synthetic lethal relationship, we next conditionally deleted *Rb1* in neuronal lineage with Nes-Cre and *Rb1*$^{lox/lox}$. Nes-Cre-mediated deletion of *Rb1* did not result in embryonic lethality on *Skp2*$^{+/+}$ (22) or *Skp2*$^{-/-}$ background (Table 2). When genotyping was performed at weaning age (21 days or older), we have not found a *Skp2*$^{-/-}$;*Nes-Cre;Rb1*$^{lox/lox}$ mouse, indicating that *Skp2*$^{-/-}$ did not rescue the neonatal lethality of *Nes-Cre;Rb1*$^{lox/lox}$ mice (22). E13.5 *Skp2*$^{+/+}$;*Nes-Cre;Rb1*$^{lox/lox}$ embryos did not contain apoptosis in the neuroepithelium of the brain (Fig. 3, *A* and *B*, *panel b*), which confirmed a previous report (22). In *Skp2*$^{-/-}$ E13.5 embryos, the same *Rb1* deletion induced massive apoptosis in the brain, detectable by TUNEL staining (Fig. 3, *B*, *panel d*, and *D*, *panel d*; quantified Fig. 3*E*), H&E staining (Fig. 3*C*, *panel d*), and staining (see Fig. 5*G*) and Western blotting (Fig. 5*D*) for cleaved (activated) Caspase 3 (aCasp3 for short). In *Rb1*$^{-/-}$ embryogenesis, E13.5 *Rb1*$^{-/-}$ embryos also showed similar neuronal apoptosis, but the apoptosis was prevented when *Rb1*$^{-/-}$ embryos were supplied with *Rb1*$^{+/+}$ placentas. *Nes-Cre;Rb1*$^{lox/lox}$ does not delete *Rb1* in placentas nor in non-neuronal tissues in embryo proper.

Apoptosis in the brain of *Rb1*$^{-/-}$ embryos was prevented by additional deletion of *Trp53* (23, 24). When we additionally

TABLE 2

***Nes-Cre;Rb1*$^{lox/lox}$;*Skp2*$^{-/-}$ embryos develop to full term**

Pregnant females were sacrificed to obtain the embryos on three different gestational days (Age column). All embryos were alive; total and expected (in parentheses) numbers for the two key genotypes are shown. These two genotypes also generated similar numbers of live newborns. Live E13.5 and E15.5 embryos are indicated by the presence of a heartbeat. Presence of movement indicate live E17.5 embryos and live newborns.

Age	Nes-Cre;Rb1$^{lox/lox}$;Skp2$^{+/+}$	Nes-Cre;Rb1$^{lox/lox}$;Skp2$^{-/-}$
E13.5	22 (15)	14 (8)
E15.5	15 (10)	12 (9)
E17.5	13 (8)	4 (3)

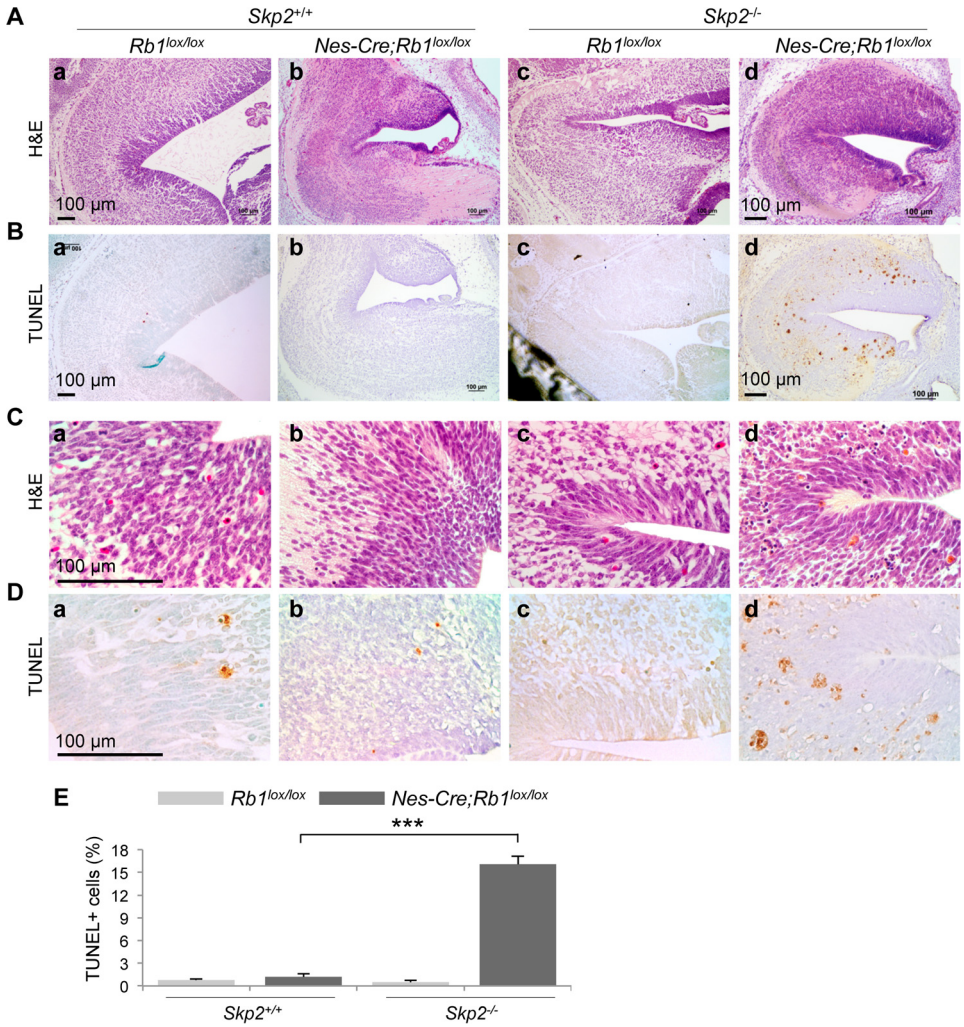

FIGURE 3. **Cell autonomous *Skp2-Rb1* synthetic lethal neuronal apoptosis on E13. 5.** *A–D*, sections of E13.5 brains of the indicated genotypes were stained with H&E (*A* and *C*) or TUNEL (*B* and *D*) and imaged at low (*A* and *B*) and high (*C* and *D*) magnifications. *E*, quantification of TUNEL staining. 400–500 cells were counted on high magnification pictures from three sets of embryos. The *bar graphs* show averages ± S.E. Statistical analyses were by Student's *t* test. ***, $p < 0.001$.

deleted *Trp53* in neuronal lineage together with *Rb1* in $Skp2^{-/-}$; $Nes\text{-}Cre;Rb1^{lox/lox};Trp53^{lox/lox}$ embryos, the brain apoptosis remained, as detected by TUNEL staining (Fig. 4, *B*, *panel b*, and *D*, *panel b*) and H&E staining (Fig. 4*C*, *panel b*). These findings demonstrate that combined deletion of *Rb1* and *Skp2* can cell autonomously induce apoptosis in neuroepithelium of the developing brain and that the underlying mechanism for this synthetic lethal apoptosis is fundamentally different from that for the non-cell autonomously induced brain apoptosis in $Rb1^{-/-}$ embryos.

Skp2-Rb1 Synthetic Lethal Neuronal Apoptosis Coexists with Further Enhanced Proliferation—To investigate the mechanisms of *Skp2-Rb1* synthetic lethal brain apoptosis, we determined how $Skp2^{-/-}$ affected the effects of *Rb1* deletion in the brain. Nes-Cre-mediated deletion of *Rb1* in embryos afforded us brain tissues to quantitatively determine E2F target gene expression by RT-qPCR and Western blot. pRb represses the activating E2F subfamily E2F1, E2F2, and E2F3, whose target genes are mostly proliferative, with E2F1 being able to additionally activate expression of apoptotic gene PUMA via ARF-p53 and p73 directly as an E2F1 target gene. Following loss of *Rb1*, expression of typical proliferative E2F target genes is increased comparing brain tissues of $Rb1^{lox/lox}$ and $Nes\text{-}Cre;Rb1^{lox/lox}$ embryos (Fig. 5*A*). Consistent with the lack of brain apoptosis in $Nes\text{-}Cre;Rb1^{lox/lox}$ embryos, expression of E2F1 apoptotic target genes was not increased (Fig. 5*B*). When we determined expression of proliferative E2F target genes in brains of $Skp2^{-/-}$; $Nes\text{-}Cre;Rb1^{lox/lox}$ embryos, we found that $Skp2^{-/-}$ did not correct the increased expression but instead increased the expression further and activated expression of E2F1 apoptotic target genes (Fig. 5, *A* and *B*). The further increased expression of proliferative E2F target genes and activation of expression of apoptotic E2F1 target genes in the brains of $Skp2^{-/-}$;*Nes-Cre*; $Rb1^{lox/lox}$ embryos were more dramatic at protein levels (Fig. 5*D*). We next show that ectopic proliferation in the intermediate zone, as measured by BrdU labeling (Fig. 5, *E* and *F*) and Western blot for pHH3 (Fig. 5*D*), is increased following *Rb1* deletion in brains of $Skp2^{+/+}$ embryos and increased further in brains of $Skp2^{-/-}$ embryos. Western blot for aCasp 3 more dramatically demonstrated *Skp2-Rb1* synthetic lethal brain apoptosis (Fig. 5*D*). These brain tissue findings indicate the cause of

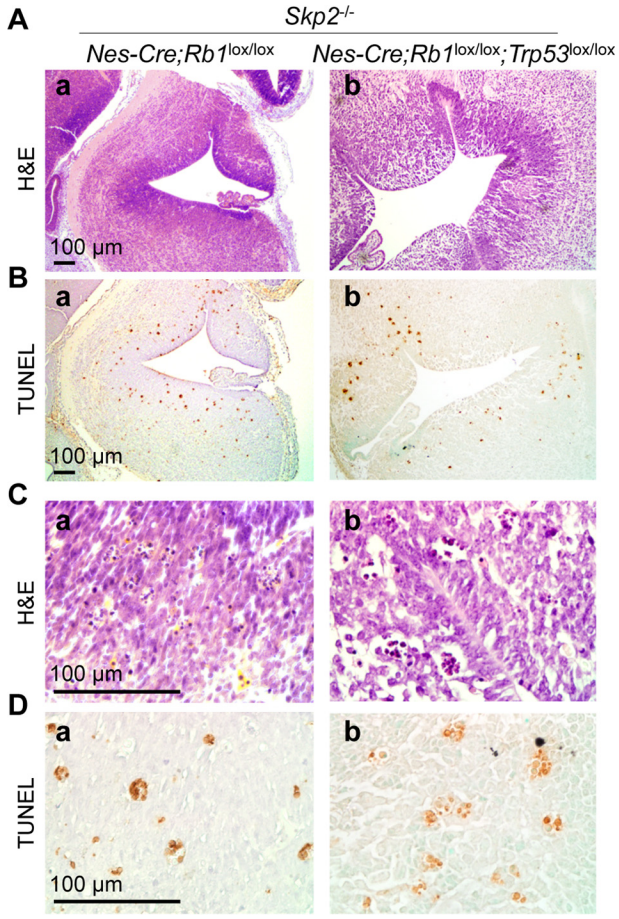

FIGURE 4. ***Skp2-Rb1* synthetic lethal neuronal apoptosis on E13. 5 is p53-independent.** As in Fig. 3, sections of E13.5 brains of the indicated genotypes were stained with H&E (*A* and *C*) or TUNEL (*B* and *D*) and imaged at low (*A* and *B*) and high (*C* and D*)* magnifications.

Skp2-Rb1 synthetic lethal neuronal apoptosis to be the further activation of E2F1.

When we additionally deleted *Trp53*, expression of its target gene PUMA was significantly reduced, whereas expression of E2F1 target gene p73 remained (Fig. 5*C*). Because the synthetic lethal neuronal apoptosis in embryonic brains is independent of p53 (Fig. 4), these findings further identify E2F1 p53-independent apoptotic activity as the underlying mechanism. Finally, most clusters of TUNEL or aCasp3-positive apoptotic cells in $Skp2^{-/-}$;*Nes-Cre*;$Rb1^{lox/lox}$ brains were doubly positive for PCNA, product of the proliferative E2F target gene (Fig. 5*G*), directly linking ectopic proliferation to the apoptosis.

Skp2-Rb1 Synthetic Lethal Neuronal Apoptosis Subsides in Late Gestation—When we determined the impact of *Skp2-Rb1* synthetic lethal brain apoptosis on brain development in $Skp2^{-/-}$;*Nes-Cre*;$Rb1^{lox/lox}$ embryos, it quickly became evident that $Skp2^{-/-}$;*Nes-Cre*;$Rb1^{lox/lox}$ embryos had normally sized brains (Fig. 6*A*) without gross structural abnormalities (Fig. 6*B*) on E18.5. To investigate the molecular basis for this lack of structural impact by the massive apoptosis seen on E13.5, we measured the expression of proliferative and apoptotic E2F target genes in brains on E13.5, E15.5, and E17.5. The sets of PCNA, E2F1, cyclin A, cyclin E (proliferative E2F target genes), p73 (apoptotic E2F1 target gene), pHH3, and aCasp3 (mitosis and apoptosis markers) that were highly expressed in the brains of $Skp2^{-/-}$;*Nes-Cre*;$Rb1^{lox/lox}$ on E13.5 became less highly expressed on E15.5 and reduced to WT levels on E17.5 (Fig. 6*C*). These findings provided a biochemical explanation for the development of the brain to normal size and structure when $Skp2^{-/-}$;*Nes-Cre*;$Rb1^{lox/lox}$ embryogenesis progressed to late gestation.

To investigate how these biochemical changes took place, we determined mRNA expression of proliferative E2F target genes as WT embryogenesis progressed to late gestation. Fig. 6*D* shows that levels of PCNA, E2F1, cyclin A, and cyclin E mRNA quickly reduced in the WT brains from E13.5. These findings suggest that mitotic exit for neuronal differentiation begins in the last 5 gestational days.

Notably, expression of Skp2 mRNA also reduced significantly in this period (Fig. 6*D*), consistent with Skp2 being an E2F target gene (5, 6). We next found that Skp2 protein levels in WT embryos also gradually reduced from E13.5 to E17.5 (Fig. 6*E*). To determine the functional impact of these reductions, we determine the protein levels of p27, because mediating p27 degradation is the best known function of Skp2. Unexpectedly, the gradual decrease in Skp2 protein levels did not induce gradual accumulation of p27 protein. Furthermore, $Skp2^{-/-}$ induced accumulation of p27 in the brain, and combined deletion of *Rb1* further increased p27 accumulation on E13.5. This two-step p27 accumulation was much reduced on E15.5 and became nonexistent on E17.5. These findings suggest that, with reduced expression, Skp2 roles in the degradation of p27 gradually became dispensable for preventing p27 protein accumulation. The reduced role of Skp2 in preventing p27 protein accumulation could be due to its reduced expression, activation of other ubiquitin ligases for p27, or, more likely, a combination of these. These findings suggest that naturally reduced expression of Skp2 and naturally increased Skp2-independent mechanisms to prevent p27 protein accumulation weakened the *Skp2-Rb1* synthetic lethal relationship when embryogenesis progressed to late gestation.

Discussion

A key strategy to study pRb is to identify its repressing targets, defined as pRb binding proteins whose functions are repressed when bound by pRb. The best established pRb repressing targets are E2F1, E2F2, and E2F3, the activator members of the E2F family. pRb binds these activator E2Fs to inhibit their transactivating functions and to recruit repressive chromatin modifiers onto the promoters of their target genes to achieve long term repression. When a pRb repressing target is functionally significant, the effects of *Rb1* deletion should be reduced when this pRb repressing target is inactivated. Indeed, pituitary tumorigenesis in $Rb1^{+/-}$ mice is inhibited in $E2f1^{-/-}$;$Rb1^{+/-}$ mice (2) or $E2f3^{-/-}$;$Rb1^{+/-}$ mice (3) and combining deletion of *E2f1* (12), *E2f2* (25), or *E2f3* (11, 13) corrected certain defects in $Rb1^{-/-}$ embryos and placentas to improve $Rb1^{-/-}$ embryogenesis. A weakness shared by these three pRb repressing targets is that their individual deletion only partially inhibited pituitary tumorigenesis in $Rb1^{+/-}$ mice. Deleting *E2f1*, *E2f2*, and *E2F3* together is embryonic lethal (26); its

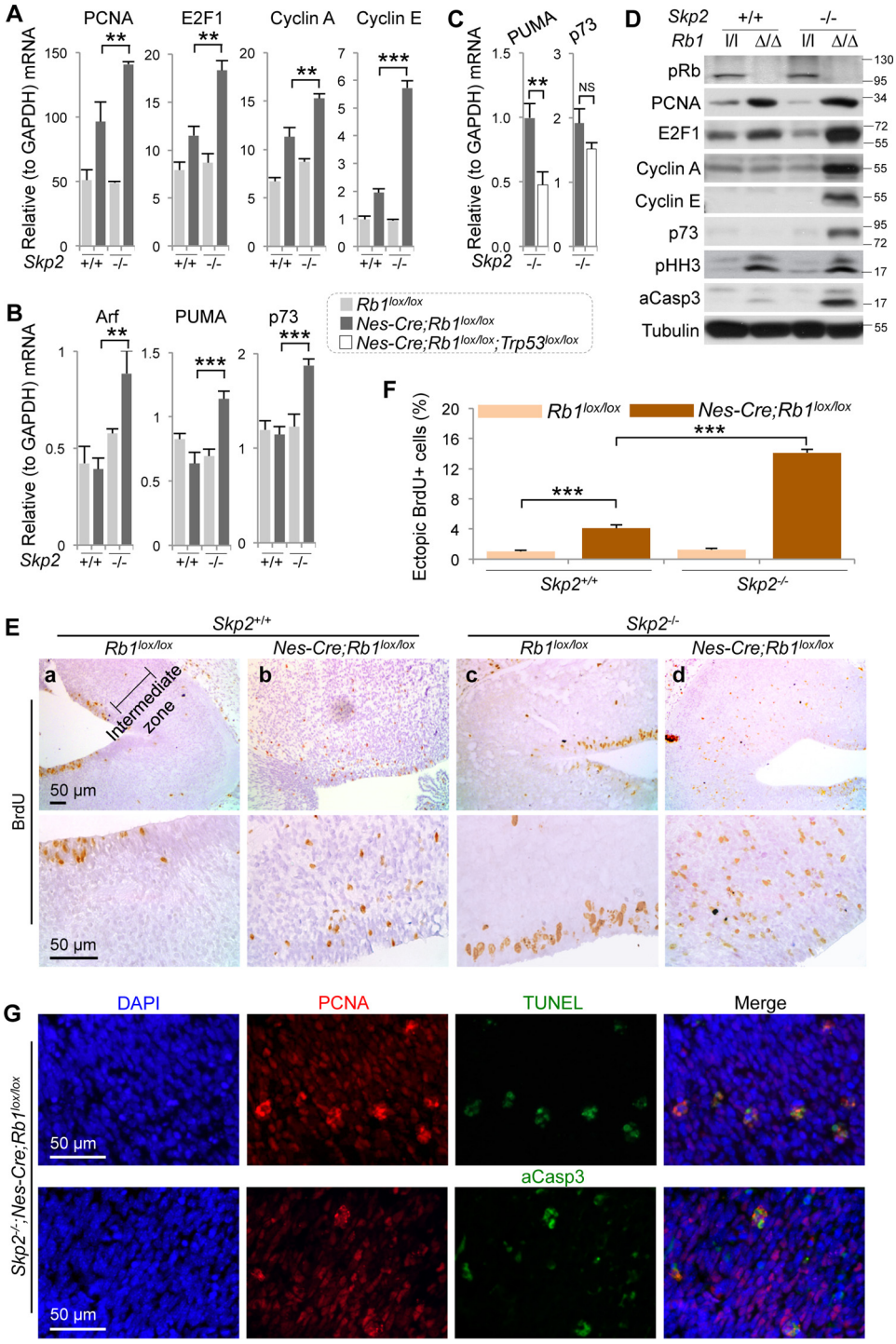

FIGURE 5. **Biochemical and further cellular analysis of *Skp2-Rb1* synthetic lethal neuronal apoptosis on E13. 5.** *A*, RT-qPCR analysis of proliferative E2F target gene expression in the brains of the indicated genotypes. *B*, same as in *A* but on apoptotic E2F target genes. *C*, same as in *B* but with an additional genotype indicated by the *white columns*. *D*, Western blots for the indicated proteins in the indicated brain tissues. Loading of lysate was equalized by protein content and demonstrated by reprobing the blots with anti-tubulin, whose levels do not change with deletions of *Rb1*, *Skp2*, or both. *l/l* indicates lox/lox, and Δ/Δ indicates deleted status of Nes-Cre;$Rb1^{lox/lox}$. Protein molecular mass markers in kDa are on the *right*. *E*, BrdU labeling of brain sections of the indicated genotypes. *F*, labeling in the intermediate zone is quantified, shown as averages ± S.E. Student's *t* test was used for statistical analysis. ***, $p < 0.001$. *G*, brain sections of $Skp2^{-/-}$;Nes-Cre;$Rb1^{lox/lox}$ embryos were co-stained with PCNA and TUNEL (*upper row*) or PCNA and aCasp3 (*lower row*), both counterstained with DAPI. *Merge* shows combined *blue*, *red*, and *green* channels. Images are representative of at least three sets of embryos.

effects on pituitary tumorigenesis in $Rb1^{+/-}$ mice remain to be tested by their conditional deletion in pituitary melanotrophs.

Skp2 is the first pRb repressing target whose deletion prevented pituitary tumorigenesis in $Rb1^{+/-}$ mice. Pomc-Cre-mediated deletion of *Rb1* in pituitary melanotrophs in $Skp2^{-/-}$ mice suggested apoptotic elimination of $Skp2^{-/-}$;$Rb1^{+/-}$ melanotrophs that lost the remaining WT allele of *Rb1*. However, Pomc-Cre-mediated deletion of *Rb1* in pituitary melanotrophs is not a physiologically relevant mechanism of *Rb1* inactivation, and the pituitary intermediate lobe is too minis-

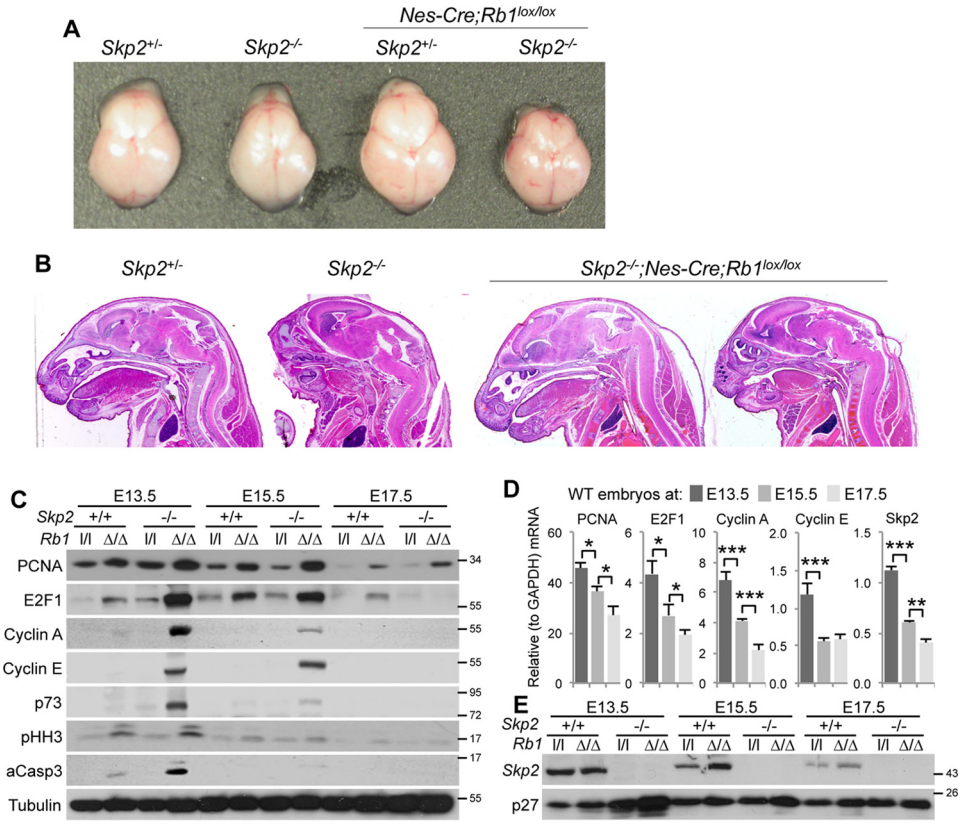

FIGURE 6. **Structural and biochemical analysis of *Skp2-Rb1* synthetic lethal neuronal apoptosis in late gestation.** *A*, pictures of a set of representative (of three for each genotypes) brains dissected out from E18.5 embryos of the indicated genotypes. *B*, H&E-stained head sections of E18.5 embryos of the indicated genotypes. *C*, Western blots, performed as in Fig. 5*D*, for the indicated proteins in brains of the indicated genotypes were labeled as in Fig. 5*D*. Three gestational ages were studied. *D*, RT-qPCR gene expression analysis of WT brains of the indicated gestational ages. *E*, Western blot analyses of Skp2 and p27 levels in brains of the indicated embryos at the indicated gestational ages. Loading control is the same as in *C*. Protein molecular mass markers in kDa are on the *right* of the blots.

cule to allow biochemical studies to understand the underlying mechanisms.

We next used cultured MEFs to study the mechanisms of apoptosis by co-deletion of *Skp2* and *Rb1* (20). As expected, acute deletion of *Rb1* in WT MEFs induced increased expression of E2F target genes. Unexpectedly, E2F target gene expression increased further when *Rb1* was deleted in $Skp2^{-/-}$ MEFs. Cyclin A binds E2F1 to repress its transactivating activity, and cyclin A is a E2F target gene; activated E2F1 following *Rb1* deletion is therefore restrained by cyclin A. $Skp2^{-/-}$ MEFs accumulate a significant amount of p27 protein, which competed against E2F1 for binding to cyclin A. The freed E2F1 is therefore "superactivated" to further increase expression of proliferation and apoptotic target genes. Remarkably, *E2f1* deletion reduced oncogenic expansion of pituitary intermediate lobe in $Skp2^{+/+}$; *Pomc-Cre;*$Rb1^{lox/lox}$ mice but increased the thickness of the pituitary intermediate lobe in $Skp2^{-/-}$*;Pomc-Cre;*$Rb1^{lox/lox}$ mice. However, important questions remained. $Skp2^{-/-}$ MEFs in culture accumulated p27 to higher degrees than most tissues in $Skp2^{-/-}$ mice, and the role of p53 in apoptosis is unclear.

In the present study, we used embryogenesis to study the functional relationship between $Skp2^{-/-}$ and $Rb1^{-/-}$. By mating $Skp2^{+/-}$*;*$Rb1^{+/-}$ mice, we have now established that $Skp2^{-/-}$ and $Rb1^{-/-}$ are synthetic lethal at the organismal level. We demonstrate that $Skp2^{-/-}$ did not inhibit ectopic proliferation in $Rb1^{-/-}$ neuroepithelium intermediate zone but induced apoptosis specifically in the neuroepithelium of $Rb1^{-/-}$ embryos. These findings provide *in vivo* evidence for a synthetic lethal relationship that is currently unique among the growing list of pRb repressing targets. By generating $Skp2^{-/-}$*;Nes-Cre;*$Rb1^{lox/lox}$ embryos, we have further established the *Skp2-Rb1* synthetic lethal relationship *in vivo* at a cell autonomous level with a biochemical understanding. In this cell autonomous setting, *Rb1* deletion activated E2Fs to increase expression of proliferative genes but not apoptotic genes; co-deletion of *Skp2* and *Rb1* not only further activated E2F proliferative target genes but activated expression of E2F1 apoptotic target genes. The role of a further activated E2F1 in this *Skp2-Rb1* synthetic lethal apoptosis is dramatically demonstrated by the findings that (i) ectopic proliferation in the neuroepithelium is further increased, (ii) most apoptotic cells expressed the proliferative marker PCNA, and (iii) the apoptosis is independent of p53.

Finally, it is evident that most other tissues in E10.5 $Skp2^{-/-}$*;* $Rb1^{-/-}$ embryos do not contain significantly increased apoptosis, thereby documenting that the *Skp2-Rb1* synthetic lethal relationship is context-dependent. Our study of brains of $Skp2^{-/-}$*;Nes-Cre;*$Rb1^{lox/lox}$ embryos in late gestation further demonstrated a number of mechanisms that could nullify *Skp2-Rb1* synthetic lethal neuronal apoptosis, including lower expression of Skp2 and developing additional mechanisms of

p27 degradation to render Skp2 dispensable in preventing p27 accumulation.

Inactivation of pRb is a highly recurrent feature of cancer cells, and inhibiting pRb repressing targets is a logical and intensively pursued therapeutic strategy for pRb-deficient cancer. The identification of *Skp2-Rb1* synthetic lethal relationship illuminated a highly attractive new strategy for pRb-deficient cancer. It is increasingly clear that cancer as an heterogeneous disease cannot be cured by a single treatment, no matter how effective it might be for certain cases. It is further evident that no matter how effective a treatment is at the beginning, cancer always evolves to resist it. The *Skp2-Rb1* synthetic lethal apoptosis in embryogenesis show these two features, and our findings suggest the cancer characteristics that are best suited for the *Skp2-Rb1* synthetic lethal treatment strategy (genetic inactivation of pRb with high expression of Skp2), how these cancers might develop resistance to this treatment (select for additional abilities to degrade p27), and how the resistant cancer might be treated (combining targeting the other p27 ubiquitin ligases).

Author Contributions—H. Z., H. W., and L. Z. conceived and coordinated the study. H. Z., H. W., F. B., Z. L., H. F., and J. C. performed the experiments. H. Z. and L. Z. wrote the paper.

Acknowledgments—We thank Dr. Keiko Nakayama and Dr. Keiich Nakayama for providing the Skp2 KO mice.

References

1. Trimarchi, J. M., and Lees, J. A. (2002) Sibling rivalry in the E2F family. *Nat. Rev. Mol. Cell Biol.* **3,** 11–20
2. Yamasaki, L., Bronson, R., Williams, B. O., Dyson, N. J., Harlow, E., and Jacks, T. (1998) Loss of E2F-1 reduces tumorigenesis and extends the lifespan of $Rb1^{+/-}$ mice. *Nat. Genet.* **18,** 360–364
3. Ziebold, U., Lee, E. Y., Bronson, R. T., and Lees, J. A. (2003) E2F3 loss has opposing effects on different pRB-deficient tumors, resulting in suppression of pituitary tumors but metastasis of medullary thyroid carcinomas. *Mol. Cell Biol.* **23,** 6542–6552
4. Ji, P., Jiang, H., Rekhtman, K., Bloom, J., Ichetovkin, M., Pagano, M., and Zhu, L. (2004) An Rb-Skp2-p27 pathway mediates acute cell cycle inhibition by Rb and is retained in a partial-penetrance Rb mutant. *Mol. Cell* **16,** 47–58
5. Zhang, L., and Wang, C. (2006) F-box protein Skp2: a novel transcriptional target of E2F. *Oncogene* **25,** 2615–2627
6. Yung, Y., Walker, J. L., Roberts, J. M., and Assoian, R. K. (2007) A Skp2 autoinduction loop and restriction point control. *J. Cell Biol.* **178,** 741–747
7. Binné, U. K., Classon, M. K., Dick, F. A., Wei, W., Rape, M., Kaelin, W. G., Jr., Näär, A. M., and Dyson, N. J. (2007) Retinoblastoma protein and anaphase-promoting complex physically interact and functionally cooperate during cell-cycle exit. *Nat. Cell Biol.* **9,** 225–232
8. Lasorella, A., Rothschild, G., Yokota, Y., Russell, R. G., and Iavarone, A. (2005) Id2 mediates tumor initiation, proliferation, and angiogenesis in Rb mutant mice. *Mol. Cell Biol.* **25,** 3563–3574
9. Jacks, T., Fazeli, A., Schmitt, E. M., Bronson, R. T., Goodell, M. A., and Weinberg, R. A. (1992) Effects of an Rb mutation in the mouse. *Nature* **359,** 295–300
10. Lee, E. Y., Chang, C.-Y., Hu, N., Wang, Y.-C., Lai, C.-C., Herrup, K., Lee, W.-H., and Bradley, A. (1992) Mice deficient for Rb are nonviable and show defects in neurogenesis and haematopoiesis. *Nature* **359,** 288–294
11. Wenzel, P. L., Wu, L., de Bruin, A., Chong, J. L., Chen, W. Y., Dureska, G., Sites, E., Pan, T., Sharma, A., Huang, K., Ridgway, R., Mosaliganti, K., Sharp, R., Machiraju, R., Saltz, J., Yamamoto, H., Cross, J. C., Robinson, M. L., and Leone, G. (2007) Rb is critical in a mammalian tissue stem cell population. *Genes Dev.* **21,** 85–97
12. Tsai, K. Y., Hu, Y., Macleod, K. F., Crowley, D., Yamasaki, L., and Jacks, T. (1998) Mutation of E2f-1 suppresses apoptosis and inappropriate S phase entry and extends survival of Rb-deficient mouse embryos. *Mol. Cell* **2,** 293–304
13. Ziebold, U., Reza, T., Caron, A., and Lees, J. A. (2001) E2F3 contributes both to the inappropriate proliferation and to the apoptosis arising in Rb mutant embryos. *Genes Dev.* **15,** 386–391
14. Lasorella, A., Noseda, M., Beyna, M., Yokota, Y., and Iavarone, A. (2000) Id2 is a retinoblastoma protein target and mediates signalling by Myc oncoproteins. *Nature* **407,** 592–598
15. Sage, J., Miller, A. L., Pérez-Mancera, P. A., Wysocki, J. M., and Jacks, T. (2003) Acute mutation of retinoblastoma gene function is sufficient for cell cycle re-entry. *Nature* **424,** 223–228
16. Nakayama, K., Nagahama, H., Minamishima, Y. A., Matsumoto, M., Nakamichi, I., Kitagawa, K., Shirane, M., Tsunematsu, R., Tsukiyama, T., Ishida, N., Kitagawa, M., Nakayama, K., and Hatakeyama, S. (2000) Targeted disruption of Skp2 results in accumulation of cyclin E and p27(Kip1), polyploidy and centrosome overduplication. *EMBO J.* **19,** 2069–2081
17. Marino, S., Vooijs, M., van Der Gulden, H., Jonkers, J., and Berns, A. (2000) Induction of medulloblastomas in p53-null mutant mice by somatic inactivation of Rb in the external granular layer cells of the cerebellum. *Genes Dev.* **14,** 994–1004
18. Wang, H., Bauzon, F., Ji, P., Xu, X., Sun, D., Locker, J., Sellers, R. S., Nakayama, K., Nakayama, K. I., Cobrinik, D., and Zhu, L. (2010) Skp2 is required for survival of aberrantly proliferating Rb1-deficient cells and for tumorigenesis in $Rb1^{+/-}$ mice. *Nat. Genet.* **42,** 83–88
19. Zhao, H., Bauzon, F., Fu, H., Lu, Z., Cui, J., Nakayama, K., Nakayama, K. I., Locker, J., and Zhu, L. (2013) Skp2 deletion unmasks a p27 safeguard that blocks tumorigenesis in the absence of pRb and p53 tumor suppressors. *Cancer Cell* **24,** 645–659
20. Lu, Z., Bauzon, F., Fu, H., Cui, J., Zhao, H., Nakayama, K., Nakayama, K. I., and Zhu, L. (2014) Skp2 suppresses apoptosis in Rb1-deficient tumours by limiting E2F1 activity. *Nat. Commun.* **5,** 3463
21. Wu, L., de Bruin, A., Saavedra, H. I., Starovic, M., Trimboli, A., Yang, Y., Opavska, J., Wilson, P., Thompson, J. C., Ostrowski, M. C., Rosol, T. J., Woollett, L. A., Weinstein, M., Cross, J. C., Robinson, M. L., and Leone, G. (2003) Extra-embryonic function of Rb is essential for embryonic development and viability. *Nature* **421,** 942–947
22. MacPherson, D., Sage, J., Crowley, D., Trumpp, A., Bronson, R. T., and Jacks, T. (2003) Conditional mutation of Rb causes cell cycle defects without apoptosis in the central nervous system. *Mol. Cell Biol.* **23,** 1044–1053
23. Morgenbesser, S. D., Williams, B. O., Jacks, T., and DePinho, R. A. (1994) p53-dependent apoptosis produced by Rb-deficiency in the developing mouse lens. *Nature* **371,** 72–74
24. Macleod, K. F., Hu, Y., and Jacks, T. (1996) Loss of Rb activates both p53-dependent and independent cell death pathways in the developing mouse nervous system. *EMBO J.* **15,** 6178–6188
25. Dirlam, A., Spike, B. T., and Macleod, K. F. (2007) Deregulated E2f-2 underlies cell cycle and maturation defects in retinoblastoma null erythroblasts. *Mol. Cell Biol.* **27,** 8713–8728
26. Chong, J. L., Wenzel, P. L., Sáenz-Robles, M. T., Nair, V., Ferrey, A., Hagan, J. P., Gomez, Y. M., Sharma, N., Chen, H. Z., Ouseph, M., Wang, S. H., Trikha, P., Culp, B., Mezache, L., Winton, D. J., Sansom, O. J., Chen, D., Bremner, R., Cantalupo, P. G., Robinson, M. L., Pipas, J. M., and Leone, G. (2009) E2f1–3 switch from activators in progenitor cells to repressors in differentiating cells. *Nature* **462,** 930–934